



Evaluation of effective connectivity of motor areas during motor imagery and execution using conditional Granger causality

Qing Gao^{a,b}, Xujun Duan^a, Huafu Chen^{a,c,*}

^a Key laboratory for Neuroinformation of Ministry of Education, School of Life Science and Technology, University of Electronic Science and Technology of China, Chengdu, 610054, PR China

^b School of Mathematical Sciences, University of Electronic Science and Technology of China, Chengdu, 610054, PR China

^c State Key Laboratory of Brain and Cognitive Science, Institute of Biophysics, Chinese Academy of Sciences, Beijing, 100101, PR China

ARTICLE INFO

Article history:

Received 1 July 2010

Revised 30 August 2010

Accepted 30 August 2010

Available online 7 September 2010

Keywords:

Conditional Granger causality

Effective connectivity

Functional magnetic resonance imaging

Motor execution

Motor imagery

ABSTRACT

The effective connectivity networks among overlapped core regions recruited by motor execution (ME) and motor imagery (MI) were explored by means of conditional Granger causality and graph-theoretic method, based on functional magnetic resonance imaging (fMRI) data. Our results demonstrated more circuits of effective connectivity among the selected seed regions during right-hand performance than during left-hand performance, implying the influences of brain asymmetry of right-handedness on effective connectivity networks. The increased causal connections were found during ME than during MI, suggesting that the ME network may have some additional connections compared to MI networks to execute the overt physical movement. Furthermore, the In–Out degrees of information flow suggested left dorsal premotor cortex (PMd), inferior parietal lobule (IPL) and superior parietal lobule (SPL) as causal sources in ME/MI tasks, highlighting the dominant function of left PMd, IPL and SPL. These findings depicted the causal connectivity of motor related core regions in fronto-parietal circuit and might indicate the conversion of causal networks between ME and MI.

© 2010 Elsevier Inc. All rights reserved.

Introduction

Motor imagery (MI), defined as internal rehearsal of a movement without any overt physical movement (Jeannerod, 1995; Porro et al., 1996), has been demonstrated beneficial in sports training (Brouziyne and Molinaro, 2005; Lotze and Halsband, 2006) and motor rehabilitation in patients with movement disorders (Kimberley et al., 2006; Malouin et al., 2004), and it plays a significantly important role in clinical and neuroscience studies. The neuronal representations of MI and motor execution (ME) have been studied intensively for years using brain imaging techniques, such as functional magnetic resonance imaging (fMRI), electroencephalogram (EEG) and positron emission tomography (PET) (Decety et al., 1994; Dechent et al., 2004; Ince et al., 2009; Lotze et al., 1999; Neuper et al., 2008; Roland et al., 1980; Solodkin et al., 2004). The studies focusing on the brain activation pattern have consistently shown similar brain regions activated during ME and MI, such as primary motor cortex (M1), supplementary motor area (SMA) and premotor cortex (PMC) in the frontal lobe and inferior parietal lobule (IPL), superior parietal lobule (SPL) and primary somatosensory cortex (S1) in the parietal lobe

(Gerardin et al., 2000; Guillot et al., 2008; Hanakawa et al., 2003; Lotze et al., 1999; Michelon et al., 2006; Roth et al., 1996; Solodkin et al., 2004; Szameitat et al., 2007).

Recently, there is a growing concern for interactions of the activated brain regions, typically in terms of ‘effective connectivity’ (Friston, 1993). Solodkin et al. (Solodkin et al., 2004) used structural equation modeling (Mohamed et al., 2003) to estimate the effective connectivity networks underlying ME, visual MI and kinesthetic MI with specified regions of interest. Their results showed that the inputs from SMA and lateral–dorsal PMC to M1, which were facilitatory during ME, had the opposite effect during kinetic MI, suggesting a physiological mechanism whereby the system prevents overt movements (Solodkin et al., 2004). More recently, dynamic causal modeling (DCM) (Friston et al., 2003) was also applied to MI task to determine effective connectivity measures between SMA and M1 (Kasess et al., 2008). The results revealed a strong suppressive influence SMA exerted on M1 during MI condition. In our prior studies, the Granger causality mapping (GCM) method has been used to analyze the effective connectivity between the left M1 (LM1) and other brain regions during ME for right-handed subjects (Gao et al., 2008), showing the effective connectivity networks between the LM1 and right M1 (RM1) and the LM1 and SMA during bimanual movement. In addition, the method has been used to explore the effective connectivity between SMA and other brain regions during MI (Chen et al., 2009). The result showed forward and backward effective connectivity between the SMA and other regions.

* Corresponding author. Key Laboratory for Neuroinformation of Ministry of Education, School of Life Science and Technology, University of Electronic Science and Technology of China, Chengdu 610054, PR China. Fax: +86 28 83208238.

E-mail address: chenhf@uestc.edu.cn (H. Chen).

In sum, the previous work had verified the effective connectivity networks among activated brain regions during ME and MI, respectively. However, the seed-based method focused on the effective connectivity between the seed region and the remaining regions, thus lacked investigation of the connectivity circuit among multiple regions involved in ME and MI. In addition, these studies focused on establishing the inter-relationships among the specifically activated areas in ME or MI. Since the distribution of activation tends to be similar in two conditions and the locations of the involved activated brain areas for ME and MI are partly overlapping (Deiber et al., 1996; Gerardin et al., 2000; Munzert et al., 2009; Solodkin et al., 2004; Stephan et al., 1995), it would be a tremendous interest to detect the conversion of the effective connectivity networks between ME and MI in the overlapped activated areas to understand the underlying neural mechanism of each condition.

In the present study, we used the Granger causality (GC) analysis and the graph-theoretic method to address the problems aforementioned. Firstly, brain activations were acquired by the general linear model (GLM) (Friston, 2004). More particularly, the overlapped parts of the activated areas in both conditions were chosen by conjunction analysis (Price and Friston, 1997) to ensure that the connectivity among the same regions of interest (ROIs) was evaluated and compared. Because of their important roles in both ME and MI (Guillot et al., 2008; Hanakawa et al., 2003; Munzert et al., 2009), ROIs were chosen from M1, SMA and dorsal premotor cortex (PMd) in the frontal lobe and from IPL, SPL and S1 in the parietal lobe. In addition, ROIs in the left SMA (LSMA) and right SMA (RSMA) were chosen separately to investigate the effective connectivity in between and to explore the different roles of SMAs related to handedness. Conditional Granger causality (CGC) method was then applied to analyze the directed influence among involved regions to distinguish the pseudo-causal relationship for three or more time series (Ding et al., 2006), instead of the GCM method used in our previous study (Chen et al., 2009). Subsequently, the nonparametric bootstrap methodology (Stilla et al., 2007) was applied to assess the statistically significant threshold of the CGC components among the regions. Besides, the information flow among the network nodes was further evaluated by the graph-theoretic method of the In–Out degrees (Jiao et al., 2010). Finally, the difference of the effective connectivity networks between ME and MI conditions in the right-/left-hand tasks was further analyzed using one-tailed two sample *t*-test.

Materials and methods

Subjects

The present study protocol was approved by the local Institutional Review Board. Twelve right-handed subjects (five females, age range 20–24 years) with no history of psychiatric or neurological illness participated in the study after giving informed consents. Handedness was evaluated by the Edinburgh Handedness Inventory (EHI). The average handedness score was 91.06, with a standard deviation of 6.01.

Experimental paradigm

The experiment was performed on a 3.0-T Siemens Trio scanner (State Key Laboratory of Brain and Cognitive Science, Institute of Biophysics, Chinese Academy of Sciences, Beijing, China) using a gradient-recalled echo planar imaging (EPI) sequence with an 8-channel head coil. The acquisition parameters were as follows: TR = 2000 ms, TE = 30 ms, FOV = 24 cm, matrix = 64 × 64, voxel size = 3.75 × 3.75 × 5 mm³, 30 transverse slices without slice gap and flip angle = 90°. High-resolution T1-weighted anatomical images were also acquired in axial orientation using a 3D spoiled gradient-recalled (SPGR) sequence. The acquisition

parameters were as follows: TR = 8.5 ms, TE = 3.4 ms, flip angle = 12°, matrix size = 512 × 512 × 156 and voxel size = 0.47 × 0.47 × 1 mm³.

The fMRI experiment performed in our previous study was repeated in the present study (Chen et al., 2009). The experiment had two runs: one for right-hand tasks and the other for left-hand tasks. Each run included 10 trials, and each trial lasted 30 seconds including 4 seconds for sequence informing, 10 seconds for MI, 6 seconds for ME and 10 seconds for resting in order. During each trial, subjects firstly learned from a visual stimulus of four sequentially presented pictures presented by a projector, indicating a random order of finger tapping, then started to imagine tapping their fingers continuously in the order that was initially informed by the visual stimulus for 10 seconds. Another cue for the next 6 seconds was presented on the screen informing the participants to perform the finger tapping exactly as they had imagined. The reason that the MI task was followed by an ME task was to ensure that the participants concentrated on the MI task and imagined the finger tapping correctly. All subjects have been trained for about one hour to perform the behavior experiments before scanning. At the end of the scanning session, the subjects were debriefed and asked about their performance of the tasks. All subjects reported performing both the ME and MI tasks successfully.

Data analyses

The acquired images were pre-processed using statistical parametric mapping (SPM) software (SPM2, <http://www.fil.ion.ucl.ac.uk/spm>). The first five images were discarded from each run to allow for magnetization equilibrium and for the subjects to get used with the circumstances. The remaining 150 images were firstly corrected for the acquisition time delay among different slices and then were realigned onto the first image for head-motion correction. In the regression model, six regressive motion correction parameters were included in the design matrix for each run as covariates with no interest. The images were then spatially normalized into a standard stereotaxic space with voxel size of 2 × 2 × 2 mm³ using the Montreal Neurological Institute (MNI) EPI template. Therefore, the voxel coordinates were transformed from the MNI coordinates to the Talairach coordinates (Talairach and Tournoux, 1988). Subsequently, a spatial smoothing filter was employed for each volume by convolving with an isotropic Gaussian kernel (FWHM = 8 mm). The statistical parametric maps (*t*-statistics) of contrasting between the ME (or MI) condition and the rest condition were generated with a threshold of $p < 0.05$ (family-wise error (FWE) corrected) to detect significantly activated brain regions during ME (or MI) condition. The conjunction analysis was applied to the *t*-maps of ME and MI to obtain the conjoint activations of the tasks (Price and Friston, 1997). A group analysis was performed to extend the inference of individual activation to the general population from which the subjects were drawn.

Identification of region of interest

The ROIs were defined as spheres within the activated regions in conjunction analysis of ME and MI conditions for each subject to ensure that the connectivity among same regions during both conditions were evaluated and compared. The spheres located in the contralateral M1 (cM1) corresponding to the performing hand, the bilateral SMA and PMd in the frontal lobe, and the contralateral S1 (cS1), bilateral IPL and SPL in the parietal lobe were selected as ROIs. The center of the sphere was at the voxel with the highest statistical value in the chosen regions. The radius of the sphere was 6 mm. The mean time course of each ROI for each subject was then calculated by averaging the time series of all voxels in the ROI. Subsequently, linear drifts were removed from the data to eliminate the effect of gross

signal drifts, which could be caused by scanner instabilities and/or gross physiological changes in the subject (Chen et al., 2009).

Signal extraction for ME and MI

To extract the signals for ME and MI conditions respectively, the mean time course was firstly deconvoluted by the classic HRF in SPM. The maximum of the delay correlation coefficient between the deconvoluted time course and the experiment pattern was then calculated to determine the time of the hemodynamic delay, which was 6 seconds. A boxcar vector was defined for each condition of interest, with the onset lagging 6 seconds after the onset of the ME or MI condition accounting for the hemodynamic delay. Finally, these boxcar vectors were multiplied with the mean time series to extract the signals for each condition separately, in light of prior studies (Cohen et al., 2005; Venkatraman et al., 2009).

The method of extracting the signals for ME and MI conditions from the mean time series was based on the GLM assumptions (Friston, 2004). According to the GLM theory, the observed time series can be modeled as a linear combination of explanatory functions, plus an error term (Friston, 2004). Specifically, in SPM, the explanatory functions constituting the design matrix are defined as the condition vectors convoluted by the HRF. Therefore, by multiplying the boxcar vectors representing the corresponding condition, the signal for each condition was successfully extracted from the mean time course of each ROI.

Conditional Granger causality analysis

In the current study, the CGC method for effective connectivity analysis was performed among the selected ROIs during ME and MI using an in-house program coded in MATLAB (The Mathworks, Natick, MA, USA). We only paid attention to the direct influence of the CGC component: the linear direct influence from x (origin) to y (target) conditional on z ($F_{x \rightarrow y|z}$). Each ROI is chosen as origin or target alternatively. When two of the ten ROIs were chosen as origin and target, the remaining eight ROIs composed of z served as conditions of the CGC analysis. The direct influence was calculated for ROIs of each subject, generating the CGC maps based on the influence measures for ME and MI conditions, and for right- and left-hand tasks, respectively.

To assess the statistical significance of CGC results, we used the framework of a nonparametric estimation based on the bootstrap methodology (Efron and Tibshirani, 1993) to obtain the null distribution for individual subject. In order to preserve the frequency content of the time series, the randomizing process was performed in the frequency domain of the time series (Stilla et al., 2007). The major steps were as follows:

- (1) Generating surrogate time series by transforming the original time series x and y into the frequency domain and randomizing their phase to be uniformly distributed over $(-\pi, \pi)$ (Kus et al., 2004; Stilla et al., 2007);
- (2) Transforming the signal back to the time domain and recalculating the CGC component $F_{x \rightarrow y|z}$;
- (3) Repeating steps (1) and (2) for M times. $M = 5000$ was used in our study.
- (4) Pooling the values of all $F_{x_i \rightarrow y_j|z}$ together to acquire the null distribution of $F_{x \rightarrow y|z}$, which is the reasonable empirical estimate under the assumption of large samples based on the law of large numbers. The p value was then defined as the $(1 - \alpha)$ quantile of the permutation samples.
- (5) Repeating steps (1), (2), (3) and (4) for all subjects.

Subsequently, the group analysis was employed using the standard meta-analysis techniques of combining p -values (Loughin, 2004). The chi-squared (2) statistical method was chosen based on the research conclusions of Loughin (2004).

In addition, the In-degree and Out-degree of the nodes in CGC causal connectivity networks were calculated for each task to evaluate the causal in/outflow connections of each node in the CGC network (Jiao et al., 2010). The In–Out degrees of the nodes, which were defined as the difference between each node's In-degree and Out-degree, were then sorted in an ascending order to identify causal target or causal source level (Jiao et al., 2010). If the In–Out degrees are the same for two nodes, the order was further sorted by the descending order of their Out-degree if the In–Out degrees < 0 or by the ascending order of their In-degree if the In–Out degrees ≥ 0 .

Results

Brain activation during tasks

The data sets of two subjects were discarded because of head movement. Fig. 1 shows the brain activation (conjunction analysis of ME and MI) during the right-hand task (Fig. 1a) and the left-hand task (Fig. 1b) obtained by the group analysis. The Talairach coordinates of peak voxels and statistical t -value for conjunction analysis of the right-hand ME and MI are reported in Table 1a, whereas Table 1b summarizes the results for the left-hand tasks.

Effective connectivity of the right-hand tasks

The average values of CGC in the right-hand ME and MI are demonstrated in Tables 2a and 2b, respectively. The row in the table represented 'target', whereas the column represented 'origin'. The asterisk showed the significant CGC components obtained by the group analysis using the standard meta-analysis techniques of combining p -values.

Fig. 2 demonstrates the networks of the statistically significant CGC components underlying right-hand ME (Fig. 2a) and MI (Fig. 2b), respectively. The red arrow represents the uni-directional connectivity, whereas the green arrow represents the bi-directional connectivity. During right-hand tasks, more effective connections existed in the left hemisphere contralateral to right hand. The results also demonstrated that the networks contained more effective connections during ME condition compared to the networks during MI condition. In the ipsilateral hemisphere, there still existed interactions between RPMd and RIPL, and between RIPL and RSPL. In the present study, the effective connectivity network between bilateral SMA and cM1 was found to be the same during ME and MI in the right-hand tasks.

The figures of the In–Out degrees of the nodes in each network were inset in Figs. 2a and b, respectively. Regardless of ME/MI task, the LSPL, LIPL and LPMd had relatively high negative In–Out degrees, whereas LS1 and LM1 had relatively high positive In–Out degrees.

Effective connectivity of left-hand tasks

The average values of CGC in the left-hand ME and MI were demonstrated in Tables 3a and 3b, respectively. The asterisk also showed the significant CGC components obtained by the group analysis.

The networks of the statistically significant CGC components underlying left-hand tasks were showed in Fig. 3. Mirror versed to right-hand tasks, more effective connections existed in the hemisphere contralateral to the left-hand tasks during both ME and MI, whereas more effective connections existed during the ME condition than those during the MI condition. There also existed interactions among ROIs in the left hemisphere, i.e., LSMA, LPMd, LIPL and LSPL, even though subjects performed unimanual tasks of the left hand. The figures of the In–Out degrees of the nodes in each network were also inset in Figs. 3a and b, respectively. The results demonstrated that in the left-hand tasks, LSPL, LPMd, IPL and RSPL had negative In–Out

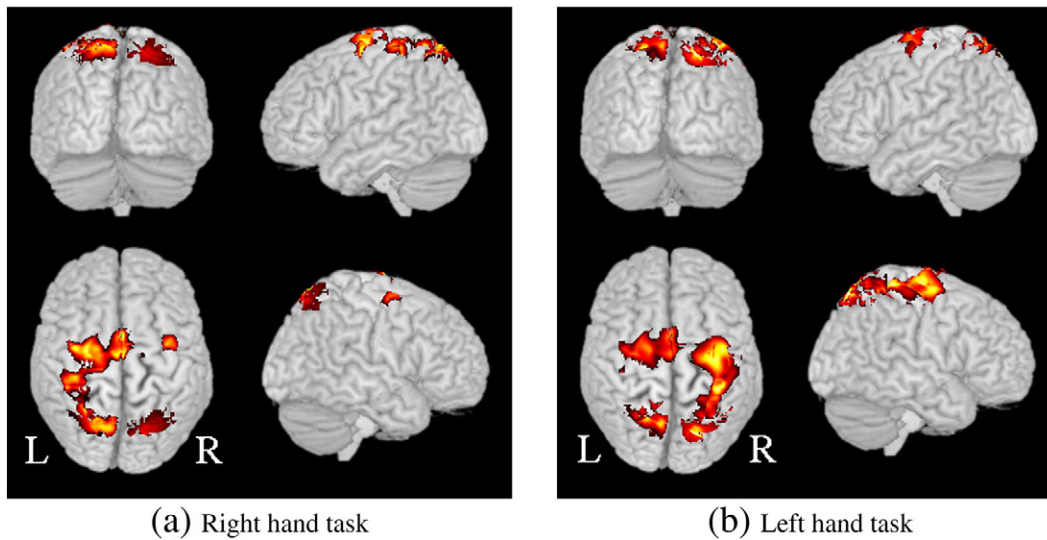


Fig. 1. The overlapped activated areas during ME and MI obtained by conjunction analysis. (a) The activated areas during right-hand tasks. The FDR-based threshold was set to $q = 0.05$ ($t\text{-value} > 3.7$). (b) The activated areas during left-hand tasks. The FDR-based threshold was set to $q = 0.05$ ($t\text{-value} > 3.5$).

degrees, whereas RS1 and RM1 had relatively high positive In–Out degrees. The effective connectivity network between bilateral SMA and cM1 was found to be mirror versed in the left-hand ME compared to that in the right-hand tasks.

Discussion

In the current study, the CGC method, which has the capability to distinguish direct from indirect connectivity among brain regions, was successfully applied to the fMRI data to explore the effective connectivity in brain regions involved in both ME and MI conditions. Our results showed the inter-regional interactions among overlapped core regions recruited in ME and MI in the frontal and parietal lobes, including cM1, cS1, bilateral SMA, PMd, IPL and SPL, expanding the prior findings of effective connectivity networks on ME and MI (Chen et al., 2009; Gao et al., 2008; Kasess et al., 2008; Solodkin et al., 2004).

Methodological considerations

GC method is an important approach to explore the dynamic causal relationships between two time series (Goebel et al., 2003; Roebroeck et al., 2005) in terms of vector autoregressive models (Geweke, 1982). However, for three or more time series, this approach has some inherent limitations. One main limitation is that

if brain regions A and B are both driven by region C but with a different lag, there will be a GC between A and B (Goebel et al., 2003; Roebroeck et al., 2005). To address this problem, CGC method has been proposed (Ding et al., 2006) and has been applied to field potential data from macaque monkeys when performing a GO/NO-GO visual pattern discrimination task (Chen et al., 2006) and human fMRI data during a face matching task (Zhou et al., 2009). More recently, we have used this method to evaluate the effective connectivity among different resting state networks (Liao et al., 2010). These studies showed CGC method achieved greater accuracy in detecting network connectivity than GC method (Ding et al., 2006; Zhou et al., 2009).

Brain activation of ME and MI

Fig. 1 showed the overlapped activated regions in ME and MI during the right-/left-hand tasks. The results were concordant with many other studies (Hanakawa et al., 2003; Lacourse et al., 2005; Lotze and Halsband, 2006; Lotze et al., 1999; Munzert et al., 2009; Nair et al., 2003; Simon et al., 2002; Solodkin et al., 2004; Szameitat et al., 2007) and confirmed the significant excitation of M1 during MI (Gerardin et al., 2000; Kasess et al., 2008; Lotze and Halsband, 2006; Lotze et al., 1999; Nair et al., 2003; Solodkin et al., 2004; Szameitat et al., 2007). The consistent activity throughout ME and MI in cM1, bilateral SMA and PMd of the frontal lobe and in cS1, bilateral IPL and SPL of the parietal lobe revealed that these regions play core roles during both ME and MI. In the present study, inter-regional

Table 1a
Local maxima of significantly activated regions during the right-hand tasks.

Coordinates			Regions	Hem	BA	t-value
X	Y	Z				
-34	-25	61	M1	L	4	8.22
-4	-8	62	SMA	L	6	9.38
2	-7	63		R	6	8.18
-35	-13	66	PMd	L	6	8.50
38	-9	64		R	6	5.17
-37	-36	60	S1	L	1/2/3	4.89
-34	-48	58	IPL	L	7/40	6.01
40	-40	46		R	7/40	3.83
-24	-64	60	SPL	L	7/40	7.06
22	-60	62		R	7/40	3.95

Abbreviations: BA = Brodmann’s area, Hem = hemisphere, L = left, M1 = primary motor cortex, PMd = dorsal premotor cortex, R = right, SMA = supplementary motor area, ME = motor execution and MI = motor imagery. Voxel coordinates are Talairach coordinates of the ROI center. The FDR-based threshold was set to $q = 0.05$ ($t\text{-value} > 3.7$).

Table 1b
Local maxima of significantly activated regions during the left-hand tasks.

Coordinates			Regions	Hem	BA	t-value
X	Y	Z				
39	-25	64	M1	R	4	8.96
-4	-8	62	SMA	L	6	7.33
2	-6	62		R	6	6.89
-34	-12	64	PMd	L	6	10.08
34	-14	64		R	6	9.86
40	-34	60	S1	R	1/2/3	5.26
-36	-40	56	IPL	L	7/40	7.88
44	-42	54		R	7/40	6.13
-25	-58	60	SPL	L	7/40	8.06
24	-60	62		R	7/40	8.63

Abbreviations are the same as in Table 1a. Voxel coordinates are also Talairach coordinates of the ROI center. The FDR-based threshold was set to $q = 0.05$ ($t\text{-value} > 3.5$).

Table 2a
The values of CGC during the right-hand ME.

		Origin									
		LM1	LSMA	RSMA	LPMd	RPMd	LS1	LIPL	RIPL	LSPL	RSPL
Target	LM1										
	LSMA	0.031*									
	RSMA	0.016	0.035*								
	LPMd	0.029*	0.035*	0.012							
	RPMd	0.038*	0.010	0.013	0.030*						
	LS1	0.030*	0.027*	0.018	0.023*	0.010					
	LIPL	0.011	0.026*	0.010	0.031*	0.010	0.011				
	RIPL	0.017	0.007	0.014	0.013	0.030*	0.008	0.033*	0.035	0.023*	0.019
	LSPL	0.029*	0.027*	0.016	0.024*	0.007	0.019	0.034*	0.016	0.010	0.022*
	RSPL	0.011	0.006	0.032*	0.017	0.012	0.015	0.023*	0.026*	0.024*	0.035*

*Significant CGC components obtained by the group analysis using the standard meta-analysis techniques of combining *p*-values.

interactions of the overlapped regions recruited by ME and MI based on the current imaging results were further explored by means of CGC method.

Conditional Granger causality networks of the right- and left-hand tasks

Our results showed that regardless of the right-/left-hand tasks, more causal connectivity existed in the hemisphere contralateral to the performing hand during the tasks. It is well known that right-hand movements activate primarily left hemispheric areas, whereas neural activity is lateralized to the right hemisphere for left-hand movements (Grefkes et al., 2008). As demonstrated in the present study, this lateralization occurred not only in the neural activity but also in the effective connectivity networks, suggesting that cortical control of the hand ME/MI is largely contralateral, and more information interchange occurs in the contralateral hemisphere (Amunts et al., 1996; Annett, 1985; Chen et al., 2009; Hugdahl and Davidson, 2003; Zeng et al., 2007). During MI, less effective connections were found compared to that during ME, implying the weaker transmission of the information among activated brain regions during MI. However, the contralateral lateralization still existed. Since MI is associated with motor preparation, anticipation, restraint, execution and learning (Deiber et al., 1998; Fadiga et al., 1999; Jeannerod, 1995; Lotze et al., 1999; Solodkin et al., 2004; Stephan and Frackowiak, 1996), some common neural representations can be anticipated between ME and MI along with similar contralateralized expression in causal networks (Guillot and Collet, 2005; Munzert et al., 2009; Solodkin et al., 2004).

Furthermore, our results found that in the unimanual task, the information exchange also occurred among SMA, PMd, IPL and SPL in the hemisphere ipsilateral to the performing hand, especially the effective connectivity circuit between PMd and IPL and between IPL and SPL. There has been an anatomical evidence of the macaque monkey showing dense connections of PMd with ipsilateral and contralateral cortical motor areas, most notably M1, parietal cortex and contralateral PMd (Dum and Strick, 2005; Lu et al., 1994; Marconi et al., 2003; Wise et al., 1997). The functional role of the parietal

cortex of the macaque monkey has been researched intensively by the group of Giacomo Rizzolatti. Their work demonstrated that both IPL and SPL receive somatosensory and visual inputs and are involved in the analysis of particular aspects of sensory information (Rizzolatti et al., 1998). Posterior areas of both SPL and IPL process predominantly visual information, whereas the anterior areas are related to somatosensory modality in SPL and to an integration of somatosensory and visual information in IPL (Caminiti et al., 1996; Rizzolatti et al., 1997, 1998). A recent study showed that SPL is more related to motor control whereas IPL is more related to motor cognition including MI (Creem-Regehr, 2009). More particularly, some studies suggested that PMd received strong inputs from the visual areas of the parietal–occipital region (Marconi et al., 2001; Simon et al., 2002). The forward and backward interactions among PMd, IPL and SPL found in our results suggested the function integration among the regions to mediate sensorimotor transformations related to visual-cued motor tasks (Adam et al., 2003; Rizzolatti et al., 1997). This function integration was found to be bilateral even in the unimanual tasks in the current study.

In addition, during left-hand tasks, more forward and backward effective connectivity existed in the left hemisphere, compared to that in the right hemisphere during right-hand tasks, suggesting the influences of the asymmetry of the right-handedness on the effective connectivity networks during ME and MI (Amunts et al., 1996; Annett, 1985; Fadiga et al., 1999; Hugdahl and Davidson, 2003; Li et al., 1996; Stinear et al., 2006; Zeng et al., 2007). The ordering of the In–Out degrees of the directional influence also demonstrated this lateralization for right-handed subjects. The results showed that LSPL, LIPL and LPMd had relatively high negative In–Out degrees both in ME and MI, suggesting them as causal sources during both conditions, regardless of the right-/left-hand tasks. Several studies verified the particular importance of LPMd and its dominance for selection and preparation of both ipsilateral and contralateral actions (Astafiev et al., 2003; Davare et al., 2006; Koch et al., 2006, 2007; Rushworth et al., 2003; Schluter et al., 2001, 1998). Some studies found LIPL dominance in imitation tasks (Muhlau et al., 2005; Tanaka and Inui,

Table 2b
The values of CGC during the right-hand MI.

		Origin									
		LM1	LSMA	RSMA	LPMd	RPMd	LS1	LIPL	RIPL	LSPL	RSPL
Target	LM1										
	LSMA	0.029*									
	RSMA	0.014	0.028*								
	LPMd	0.028*	0.019	0.012							
	RPMd	0.010	0.014	0.019	0.028*						
	LS1	0.016	0.025*	0.011	0.026*	0.008					
	LIPL	0.015	0.010	0.012	0.030	0.010	0.019				
	RIP	0.013	0.010	0.015	0.010	0.030*	0.014	0.028*			
	LSPL	0.019	0.024*	0.009	0.023*	0.008	0.013	0.029*	0.006	0.010	0.025*
	RSPL	0.006	0.008	0.016	0.010	0.019	0.008	0.013	0.030*	0.026*	0.016

*Significant CGC components obtained by the group analysis using the standard meta-analysis techniques of combining *p*-values.

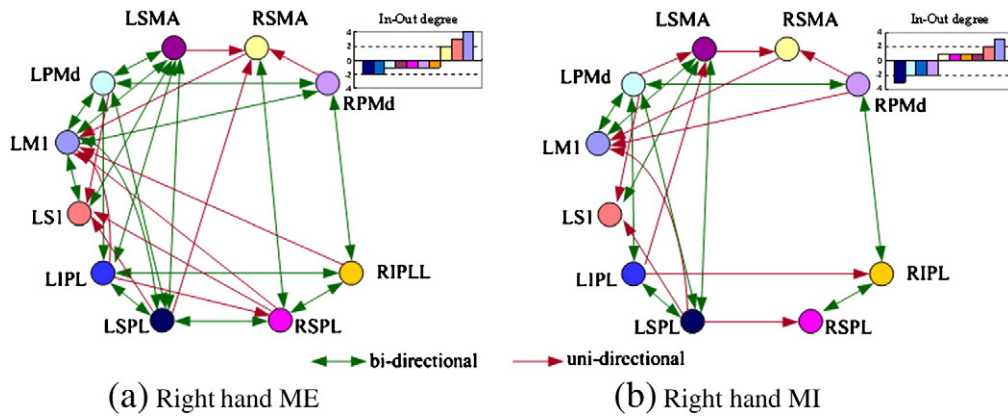


Fig. 2. The networks of the statistically significant CGC components underlying right-hand tasks. (a) Results during ME condition. (b) Results during MI condition. The green arrow represents the bi-directional connectivity, whereas the red arrow represents the uni-directional connectivity. Insets are the In–Out degrees of the nodes in each network. Abbreviations: IPL=inferior parietal lobule, L=left, M1=primary motor cortex, PMd=dorsal premotor cortex, R=right, S1=primary somatosensory cortex, SMA=supplementary motor area, SPL=superior parietal lobule.

2002; Tanaka et al., 2001). Our findings extended these findings from the point of view of the causal source, implying that LPMd, LIPL and LSPL had the dominant function during both ME and MI in right-/left-hand tasks.

Difference of conditional Granger causality networks between ME and MI

To further detect the difference of CGC networks between ME and MI, one-tailed two sample *t*-test was applied with the FWE-corrected threshold of $q = 0.01$. Fig. 4 demonstrates the significantly stronger effective connectivity networks in ME compared with MI for the right-hand (Fig. 4a) and left-hand tasks (Fig. 4b), respectively. However, significantly stronger effective connectivity in MI compared with ME was not found in the present study. The results demonstrated that regardless of the right-/left-hand task, the effective connectivity increased during ME compared to that during MI, suggesting more information exchange during ME than MI in the overlapped activated areas. Moreover, the activated results of ME and MI based on the statistical parametric maps (*t*-statistics) demonstrated that the univariate *t*-values were consistently larger in certain brain regions for ME as compared to MI (values not shown). Jeannerod (2001) developed the simulation theory postulated every overtly executed action that implies the existence of a covert stage, whereas a covert action does not necessarily turns out into an overt action (Jeannerod, 2001). Since MI is the covert stage of an action, whereas ME implies additional processes for the overt behavior stage (Munzert et al., 2009), there are both additional connections and increased activation during ME to execute the overt physical movement compared to MI.

Note the forward and backward effective circuit between cS1 and cM1 (green bi-directional arrow) in Fig. 4. The results suggested the significantly increased interactions between cS1 and cM1 during ME condition, regardless of the right-/left-hand task. S1 has classically been considered as specifically involved in the personal experience of somatic sensations (Bufalari et al., 2007), while M1 plays a significant role in sensory processing for the purpose of upcoming movement generation (Georgopoulos, 2000; Hanakawa et al., 2003). The increased forward and backward interactions between S1 and M1 during ME suggested the stronger somatosensory–motor integration between S1 and M1 during ME than during MI to achieve a more effective functional coupling in motor system during ME. Though the inter-connections between cS1 and cM1 during MI did not meet the significant threshold, the results consistently showed that they both had relatively high positive In–Out degrees during ME and MI, suggesting them as causal targets in both conditions.

Conditional Granger causality networks of bilateral SMAs

In the present study, the results showed directed influence from LSMA to RSMA in the right-hand tasks (the mirror versed result was found in the left-hand ME). The anatomic studies had reported that SMAs were reciprocally connected and each projected to both contralateral and ipsilateral primary motor areas (Muakkassa and Strick, 1979; Pandya and Vignolo, 1971), which anatomically supported our results on the functional interactions of bilateral SMA.

Furthermore, the forward and backward circuit between SMA and cM1 was found to be specifically located in the same hemisphere contralateral to the performing hand. However, for ipsilateral SMA, there existed only the causal connectivity from SMA to cM1 but no feedback from cM1 to ipsilateral SMA. The activation of both SMAs

Table 3a
The values of CGC during the left-hand ME.

		Origin									
		RM1	LSMA	RSMA	LPMd	RPMd	RS1	LIPL	RIPL	LSPL	RSPL
Target	RM1		0.038*	0.041*	0.031*	0.042*	0.032*	0.016	0.038*	0.023*	0.032*
	LSMA	0.020		0.032*	0.026*	0.015	0.010	0.019	0.011	0.024*	0.013
	RSMA	0.035*	0.021		0.008	0.034*	0.033*	0.008	0.023*	0.014	0.024*
	LPMd	0.017	0.032*	0.012		0.018	0.014	0.039*	0.008	0.036*	0.013
	RPMd	0.038*	0.018	0.037*	0.041*		0.021	0.017	0.038*	0.008	0.036*
	RS1	0.057*	0.012	0.040*	0.009	0.038*		0.013	0.013	0.025*	0.028*
	LIPL	0.009	0.010	0.011	0.031*	0.008	0.007		0.019	0.040*	0.012
	RIPL	0.009	0.015	0.029*	0.020	0.034*	0.010	0.039*		0.007	0.026*
	LSPL	0.008	0.033*	0.035*	0.024*	0.009	0.011	0.041*	0.009		0.031*
	RSPL	0.036*	0.009	0.038*	0.008	0.042*	0.019	0.011	0.039*	0.037*	

*Significant CGC components obtained by the group analysis using the standard meta-analysis techniques of combining *p*-values.

Table 3b
The values of CGC during the left-hand MI.

		Origin									
		RM1	LSMA	RSMA	LPMd	RPMd	RS1	LIPL	RIPL	LSPL	RSPL
Target	RM1		0.033*	0.031*	0.022	0.036*	0.014	0.012	0.021	0.014	0.023*
	LSMA	0.019		0.010	0.035*	0.008	0.006	0.017	0.011	0.025*	0.009
	RSMA	0.017	0.014		0.010	0.036*	0.015	0.010	0.023*	0.009	0.028*
	LPMd	0.018	0.031*	0.016		0.020	0.008	0.025*	0.011	0.036*	0.013
	RPMd	0.035*	0.015	0.012	0.035*		0.009	0.012	0.030*	0.011	0.027*
	RS1	0.015	0.018	0.030*	0.013	0.008		0.008	0.012	0.009	0.024*
	LIPL	0.005	0.007	0.012	0.026*	0.009	0.007		0.016	0.029*	0.019
	RIPL	0.009	0.010	0.017	0.008	0.033*	0.011	0.031*		0.009	0.027*
	LSPL	0.007	0.013	0.006	0.027*	0.006	0.006	0.034*	0.005		0.017
	RSPL	0.028*	0.010	0.031*	0.008	0.010	0.09	0.007	0.034*	0.023*	

*Significant CGC components obtained by the group analysis using the standard meta-analysis techniques of combining *p*-values.

may appropriately modulate M1 activity, both mediating the intended action and suppressing the unintended action during coordinated movements (Kasess et al., 2008). Our finding expanded the prior studies of the interactions between SMA and cM1 (Chen et al., 2009; Kasess et al., 2008; Solodkin et al., 2004; Babiloni et al., 2003; Gao et al., 2008; Rogers et al., 2004; Wen et al., 2006) by dividing SMA into left and right parts, implying that ipsilateral and contralateral SMAs play different roles on cM1. Further study is needed to specify the role of ipsilateral and contralateral SMAs, respectively.

Conclusions

The present study chose overlapped activated brain areas in ME and MI to detect the effective connectivity networks among involved regions in the frontal and parietal lobes by means of CGC analysis and graph-theoretic method. In our results, both the effective connectivity networks and the In-Out degrees consistently demonstrated the left lateralization for right-handed subjects. Our findings further provide evidence of the simulation theory proposed by Jeannerod (2001) in the overlapped activated regions of ME and MI, i.e., ME has some increased causal connections because of additional processes for the overt behavior stage (Munzert et al., 2009). In addition, by choosing ROI in LSMA and RSMA separately, our results implied different functions of ipsilateral SMA and contralateral SMA on cM1 during unimanual task. Future work may choose a distinct part of the activated regions instead of the overlapped part to study the effective connectivity networks of ME and MI, respectively, and to find specific roles of the involved regions during ME and MI, respectively. Furthermore, the experiment on left-handed subjects may be performed to identify the causal networks of ME and MI associated with handedness.

Acknowledgments

The authors are grateful to the anonymous referee for the constructive and helpful comments which greatly improved the manuscript. This work was supported by grants from the Natural Science Foundation of China (90820006, 61035006 and 30900326) and by an open project of the State Key Laboratory of Brain and Cognitive Science Chinese Academy of Sciences (08B08).

Appendix. Calculation of conditional Granger causality

Ding et al. (2006) has proposed the conditional Granger causality to resolve whether the interaction between two time series is direct or mediated by recorded time series. Consider three time series X_t , Y_t and Z_t , in which a pairwise Granger causality analysis reveals a causal influence from Y_t to X_t . To examine whether this influence has a direct component or is mediated entirely by Z_t , firstly the joint autoregressive representation of X_t and Z_t is modeled as follows (Ding et al., 2006):

$$X_t = \sum_{j=1}^{\infty} a_{1j}X_{t-j} + \sum_{j=1}^{\infty} b_{1j}Z_{t-j} + \varepsilon_{1t} \tag{1}$$

$$Z_t = \sum_{j=1}^{\infty} c_{1j}X_{t-j} + \sum_{j=1}^{\infty} d_{1j}Z_{t-j} + \gamma_{1t} \tag{2}$$

where the noise terms are uncorrelated over time, and their contemporaneous covariance matrix is as follows:

$$\Sigma_t = \begin{pmatrix} \Lambda_1 & T_1 \\ T_1 & \Gamma_1 \end{pmatrix} \tag{3}$$

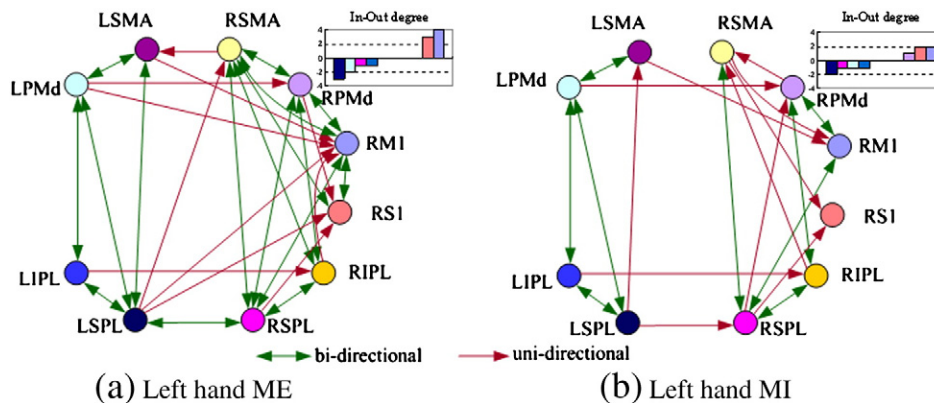


Fig. 3. The networks of the statistically significant CGC components underlying left-hand tasks. (a) Results during ME condition. (b) Results during MI condition. Insets are the In-Out degrees of the nodes in each network.

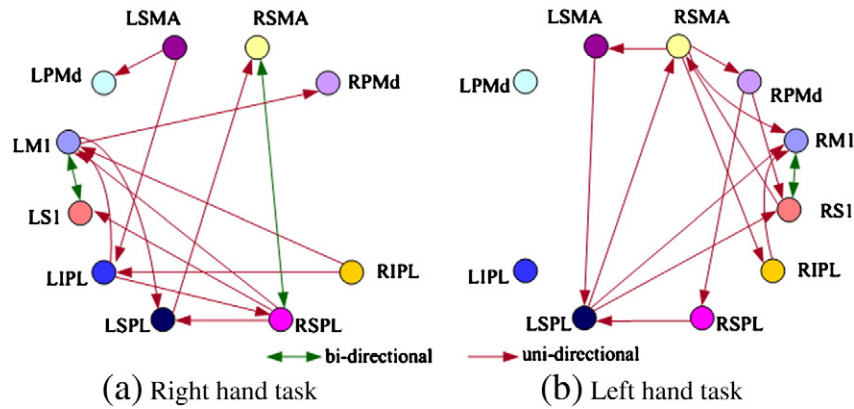


Fig. 4. The significantly stronger effective connectivity networks in ME compared with MI during (a) right-hand tasks; (b) left-hand tasks. The two sample *t*-test was used with the FWE-corrected threshold of $q = 0.01$.

Then consider the joint autoregressive representation of all three processes X_t , Y_t and Z_t :

$$X_t = \sum_{j=1}^{\infty} a_{2j} X_{t-j} + \sum_{j=1}^{\infty} b_{2j} Y_{t-j} + \sum_{j=1}^{\infty} c_{2j} Z_{t-j} + \varepsilon_{2t} \quad (4)$$

$$Y_t = \sum_{j=1}^{\infty} d_{2j} X_{t-j} + \sum_{j=1}^{\infty} e_{2j} Y_{t-j} + \sum_{j=1}^{\infty} f_{2j} Z_{t-j} + \eta_{2t} \quad (5)$$

$$Z_t = \sum_{j=1}^{\infty} u_{2j} X_{t-j} + \sum_{j=1}^{\infty} v_{2j} Y_{t-j} + \sum_{j=1}^{\infty} w_{2j} Z_{t-j} + \gamma_{2t} \quad (6)$$

where the covariance matrix of the noise terms is as follows:

$$\Sigma_2 = \begin{pmatrix} \Gamma_{xx} & \Gamma_{xy} & \Gamma_{xz} \\ \Gamma_{yx} & \Gamma_{yy} & \Gamma_{yz} \\ \Gamma_{zx} & \Gamma_{zy} & \Gamma_{zz} \end{pmatrix} \quad (7)$$

The Granger causality from Y_t to X_t conditional on Z_t is defined to be as follows:

$$F_{y \rightarrow x|z} = \ln \frac{\Lambda_1}{\Gamma_{xx}} \quad (8)$$

The meaning of this definition is the generalization of the pairwise Granger causality. When the causal influence from Y_t to X_t is entirely mediated by Z_t , $\{b_{2j}\}$ is uniformly zero, and $\Gamma_{xx} = \Lambda_1$. Therefore, we have $F_{y \rightarrow x|z} = 0$, meaning that no further improvement in the prediction of X_t can be expected by including past measurements of Y_t (Ding et al., 2006). When there is still a direct component from Y_t to X_t , the inclusion of past measurements of Y_t in addition to that of X_t and Z_t results in better predictions of X_t (Ding et al., 2006). We have $\Gamma_{xx} < \Lambda_1$, and thereby $F_{y \rightarrow x|z} > 0$.

References

Adam, J.J., Backes, W., Rijcken, J., Hofman, P., Kuipers, H., Jolles, J., 2003. Rapid visuomotor preparation in the human brain: a functional MRI study. *Brain Res. Cogn. Brain Res.* 16, 1–10.

Amunts, K., Schlaug, G., Schleicher, A., Steinmetz, H., Dabringhaus, A., Roland, P.E., Zilles, K., 1996. Asymmetry in the human motor cortex and handedness. *Neuroimage* 4, 216–222.

Annett, M., 1985. *Left, Right, Hand, Brain: The Right Shift Theory*. Lawrence Erlbaum Associates, Hove, U.K.

Astafiev, S.V., Shulman, G.L., Stanley, C.M., Snyder, A.Z., Van Essen, D.C., Corbetta, M., 2003. Functional organization of human intraparietal and frontal cortex for attending, looking, and pointing. *J. Neurosci.* 23, 4689–4699.

Babiloni, C., Carducci, F., Del Gratta, C., Demartin, M., Romani, G.L., Babiloni, F., Rossini, P.M., 2003. Hemispherical asymmetry in human SMA during voluntary simple unilateral movements. An fMRI study. *Cortex* 39, 293–305.

Brouziyne, M., Molinaro, C., 2005. Mental imagery combined with physical practice of approach shots for golf beginners. *Percept. Mot. Skills* 101, 203–211.

Bufalari, I., Aprile, T., Avenanti, A., Di Russo, F., Aglioti, S.M., 2007. Empathy for pain and touch in the human somatosensory cortex. *Cereb. Cortex* 17, 2553–2561.

Caminiti, R., Ferraina, S., Johnson, P.B., 1996. The sources of visual information to the primate frontal lobe: a novel role for the superior parietal lobule. *Cereb. Cortex* 6, 319–328.

Chen, Y., Bressler, S.L., Ding, M., 2006. Frequency decomposition of conditional Granger causality and application to multivariate neural field potential data. *J. Neurosci. Methods* 150, 228–237.

Chen, H., Yang, Q., Liao, W., Gong, Q., Shen, S., 2009. Evaluation of the effective connectivity of supplementary motor areas during motor imagery using Granger causality mapping. *Neuroimage* 47, 1844–1853.

Cohen, M.X., Heller, A.S., Ranganath, C., 2005. Functional connectivity with anterior cingulate and orbitofrontal cortices during decision-making. *Brain Res. Cogn. Brain Res.* 23, 61–70.

Creem-Regehr, S.H., 2009. Sensory-motor and cognitive functions of the human posterior parietal cortex involved in manual actions. *Neurobiol. Learn. Mem.* 91, 166–171.

Davare, M., Andres, M., Cosnard, G., Thonnard, J.L., Olivier, E., 2006. Dissociating the role of ventral and dorsal premotor cortex in precision grasping. *J. Neurosci.* 26, 2260–2268.

Decety, J., Perani, D., Jeannerod, M., Bettinardi, V., Tadary, B., Woods, R., Mazziotta, J.C., Fazio, F., 1994. Mapping motor representations with positron emission tomography. *Nature* 371, 600–602.

Dechent, P., Merboldt, K.D., Frahm, J., 2004. Is the human primary motor cortex involved in motor imagery? *Brain Res. Cogn. Brain Res.* 19, 138–144.

Deiber, M.P., Ibanez, V., Sadato, N., Hallett, M., 1996. Cerebral structures participating in motor preparation in humans: a positron emission tomography study. *J. Neurophysiol.* 75, 233–247.

Deiber, M.P., Ibanez, V., Honda, M., Sadato, N., Raman, R., Hallett, M., 1998. Cerebral processes related to visuomotor imagery and generation of simple finger movements studied with positron emission tomography. *Neuroimage* 7, 73–85.

Ding, M., Chen, Y., Bressler, S.L., 2006. *Granger Causality: Basic Theory and Application to Neuroscience*. Wiley-VCH Verlag.

Dum, R.P., Strick, P.L., 2005. Frontal lobe inputs to the digit representations of the motor areas on the lateral surface of the hemisphere. *J. Neurosci.* 25, 1375–1386.

Efron, B., Tibshirani, R.J., 1993. *An Introduction to the Bootstrap*. Chapman and Hall, New York.

Fadiga, L., Buccino, G., Craighero, L., Fogassi, L., Gallese, V., Pavesi, G., 1999. Corticospinal excitability is specifically modulated by motor imagery: a magnetic stimulation study. *Neuropsychologia* 37, 147–158.

Friston, K.J., 1993. Time-dependent changes in effective connectivity measured with PET. *Hum. Brain Mapp.* 13, 69–79.

Friston, K.J., 2004. *Introduction: Experimental Design and Statistical Parametric Mapping*. Academic Press.

Friston, K.J., Harrison, L., Penny, W., 2003. Dynamic causal modelling. *Neuroimage* 19, 1273–1302.

Gao, Q., Chen, H., Gong, Q., 2008. Evaluation of the effective connectivity of the dominant primary motor cortex during bimanual movement using Granger causality. *Neurosci. Lett.* 443, 1–6.

Georgopoulos, A.P., 2000. Neural aspects of cognitive motor control. *Curr. Opin. Neurobiol.* 10, 238–241.

Gerardin, E., Sirigu, A., Lehericy, S., Poline, J.B., Gaymard, B., Marsault, C., Agid, Y., Le Bihan, D., 2000. Partially overlapping neural networks for real and imagined hand movements. *Cereb. Cortex* 10, 1093–1104.

Geweke, J.F., 1982. Measurement of linear dependence and feedback between multiple time series. *J. Am. Stat. Assoc.* 77, 304–313.

Goebel, R., Roebroeck, A., Kim, D.S., Formisano, E., 2003. Investigating directed cortical interactions in time-resolved fMRI data using vector autoregressive modeling and Granger causality mapping. *Magn. Reson. Imaging* 21, 1251–1261.

Grefkes, C., Eickhoff, S.B., Nowak, D.A., Dafotakis, M., Fink, G.R., 2008. Dynamic intra- and interhemispheric interactions during unilateral and bilateral hand movements assessed with fMRI and DCM. *Neuroimage* 41, 1382–1394.

Guillot, A., Collet, C., 2005. Contribution from neurophysiological and psychological methods to the study of motor imagery. *Brain Res. Brain Res. Rev.* 50, 387–397.

- Guillot, A., Collet, C., Nguyen, V.A., Malouin, F., Richards, C., Doyon, J., 2008. Functional neuroanatomical networks associated with expertise in motor imagery. *Neuroimage* 41, 1471–1483.
- Hanakawa, T., Immisch, I., Toma, K., Dimyan, M.A., Van Gelderen, P., Hallett, M., 2003. Functional properties of brain areas associated with motor execution and imagery. *J. Neurophysiol.* 89, 989–1002.
- Hugdahl, K., Davidson, R.J., 2003. *The Asymmetrical Brain*. MIT Press, Cambridge, Mass.
- Ince, N.F., Goksu, F., Tewfik, A.H., Arica, S., 2009. Adapting subject specific motor imagery EEG patterns in space–time–frequency for a brain computer interface. *Biomed. Signal Process. Control* 4, 236–246.
- Jeannerod, M., 1995. Mental imagery in the motor context. *Neuropsychologia* 33, 1419–1432.
- Jeannerod, M., 2001. Neural simulation of action: a unifying mechanism for motor cognition. *Neuroimage* 14, S103–S109.
- Jiao, Q., Lu, G., Zhang, Z., Zhong, Y., Wang, Z., Guo, Y., Li, K., Ding, M., Liu, Y., 2010. Granger causal influence predicts BOLD activity levels in the default mode network. *Hum. Brain Mapp.* doi:10.1002/hbm.21065.
- Kassess, C.H., Windischberger, C., Cunnington, R., Lanzenberger, R., Pezawas, L., Moser, E., 2008. The suppressive influence of SMA on M1 in motor imagery revealed by fMRI and dynamic causal modeling. *Neuroimage* 40, 828–837.
- Kimberley, T.J., Khandekar, G., Skrabka, L.L., Spencer, J.A., Van Gorp, E.A., Walker, S.R., 2006. Neural substrates for motor imagery in severe hemiparesis. *Neurorehabil. Neural Repair* 20, 268–277.
- Koch, G., Franca, M., Del Olmo, M.F., Cheeran, B., Milton, R., Alvarez Saurco, M., Rothwell, J.C., 2006. Time course of functional connectivity between dorsal premotor and contralateral motor cortex during movement selection. *J. Neurosci.* 26, 7452–7459.
- Koch, G., Franca, M., Mochizuki, H., Marconi, B., Caltagirone, C., Rothwell, J.C., 2007. Interactions between pairs of transcranial magnetic stimuli over the human left dorsal premotor cortex differ from those seen in primary motor cortex. *J. Physiol.* 578, 551–562.
- Kus, R., Kaminski, M., Blinowska, K.J., 2004. Determination of EEG activity propagation: pair-wise versus multichannel estimate. *IEEE Trans. Biomed. Eng.* 51, 1501–1510.
- Lacourse, M.G., Orr, E.L., Cramer, S.C., Cohen, M.J., 2005. Brain activation during execution and motor imagery of novel and skilled sequential hand movements. *Neuroimage* 27, 505–519.
- Li, A., Yetkin, F.Z., Cox, R., Haughton, V.M., 1996. Ipsilateral hemisphere activation during motor and sensory tasks. *AJNR Am. J. Neuroradiol.* 17, 651–655.
- Liao, W., Mantini, D., Zhang, Z., Pan, Z., Ding, J., Gong, Q., Yang, Y., Chen, H., 2010. Evaluating the effective connectivity of resting state networks using conditional Granger causality. *Biol. Cybern.* 102, 57–69.
- Lotze, M., Halsband, U., 2006. Motor imagery. *J. Physiol. Paris* 99, 386–395.
- Lotze, M., Montoya, P., Erb, M., Hulsmann, E., Flor, H., Klose, U., Birbaumer, N., Grodd, W., 1999. Activation of cortical and cerebellar motor areas during executed and imagined hand movements: an fMRI study. *J. Cogn. Neurosci.* 11, 491–501.
- Loughin, T.M., 2004. A systematic comparison of methods for combining *p*-values from independent tests. *Comput. Stat. Data Anal.* 47, 467–485.
- Lu, M.T., Preston, J.B., Strick, P.L., 1994. Interconnections between the prefrontal cortex and the premotor areas in the frontal lobe. *J. Comp. Neurol.* 341, 375–392.
- Malouin, F., Richards, C.L., Doyon, J., Desrosiers, J., Belleville, S., 2004. Training mobility tasks after stroke with combined mental and physical practice: a feasibility study. *Neurorehabil. Neural Repair* 18, 66–75.
- Marconi, B., Genovesio, A., Battaglia-Mayer, A., Ferraina, S., Squatrito, S., Molinari, M., Lacquaniti, F., Caminiti, R., 2001. Eye–hand coordination during reaching. I. Anatomical relationships between parietal and frontal cortex. *Cereb. Cortex* 11, 513–527.
- Marconi, B., Genovesio, A., Giannetti, S., Molinari, M., Caminiti, R., 2003. Callosal connections of dorso-lateral premotor cortex. *Eur. J. Neurosci.* 18, 775–788.
- Michelon, P., Vettel, J.M., Zacks, J.M., 2006. Lateral somatotopic organization during imagined and prepared movements. *J. Neurophysiol.* 95, 811–822.
- Mohamed, M.A., Yousem, D.M., Tekes, A., Browner, N.M., Calhoun, V.D., 2003. Timing of cortical activation: a latency-resolved event-related functional MR imaging study. *AJNR Am. J. Neuroradiol.* 24, 1967–1974.
- Muakkassa, K.F., Strick, P.L., 1979. Frontal lobe inputs to primate motor cortex: evidence for four somatotopically organized ‘premotor’ areas. *Brain Res.* 177, 176–182.
- Muhlau, M., Hermsdörfer, J., Goldenberg, G., Wohlschläger, A.M., Castrop, F., Stahl, R., Rottinger, M., Erhard, P., Haslinger, B., Ceballos-Baumann, A.O., Conrad, B., Boecker, H., 2005. Left inferior parietal dominance in gesture imitation: an fMRI study. *Neuropsychologia* 43, 1086–1098.
- Munzert, J., Lorey, B., Zentgraf, K., 2009. Cognitive motor processes: the role of motor imagery in the study of motor representations. *Brain Res. Rev.* 60, 306–326.
- Nair, D.G., Purcott, K.L., Fuchs, A., Steinberg, F., Kelso, J.A., 2003. Cortical and cerebellar activity of the human brain during imagined and executed unimanual and bimanual action sequences: a functional MRI study. *Brain Res. Cogn. Brain Res.* 15, 250–260.
- Neuper, C., Scherer, R., Grieshofer, P., Pfurtscheller, G., 2008. Event-related EEG characteristics during motor imagery. *Int. J. Psychophysiol.* 69, 181–182.
- Pandya, D.N., Vignolo, L.A., 1971. Intra- and interhemispheric projections of the precentral, premotor and arcuate areas in the rhesus monkey. *Brain Res.* 26, 217–233.
- Porro, C.A., Francescato, M.P., Cettolo, V., Diamond, M.E., Baraldi, P., Zuiani, C., Bazzocchi, M., di Prampero, P.E., 1996. Primary motor and sensory cortex activation during motor performance and motor imagery: a functional magnetic resonance imaging study. *J. Neurosci.* 16, 7688–7698.
- Price, C.J., Friston, K.J., 1997. Cognitive conjunction: a new approach to brain activation experiments. *Neuroimage* 5, 261–270.
- Rizzolatti, G., Fogassi, L., Gallese, V., 1997. Parietal cortex: from sight to action. *Curr. Opin. Neurobiol.* 7, 562–567.
- Rizzolatti, G., Luppino, G., Matelli, M., 1998. The organization of the cortical motor system: new concepts. *Electroencephalogr. Clin. Neurophysiol.* 106, 283–296.
- Roebroeck, A., Formisano, E., Goebel, R., 2005. Mapping directed influence over the brain using Granger causality and fMRI. *Neuroimage* 25, 230–242.
- Rogers, B.P., Carew, J.D., Meyerand, M.E., 2004. Hemispheric asymmetry in supplementary motor area connectivity during unilateral finger movements. *Neuroimage* 22, 855–859.
- Roland, P.E., Larsen, B., Lassen, N.A., Skinhoj, E., 1980. Supplementary motor area and other cortical areas in organization of voluntary movements in man. *J. Neurophysiol.* 43, 118–136.
- Roth, M., Decety, J., Raybaudi, M., Massarelli, R., Delon-Martin, C., Segebarth, C., Morand, S., Gemignani, A., Decors, M., Jeannerod, M., 1996. Possible involvement of primary motor cortex in mentally simulated movement: a functional magnetic resonance imaging study. *Neuroreport* 7, 1280–1284.
- Rushworth, M.F., Johansen-Berg, H., Gobel, S.M., Devlin, J.T., 2003. The left parietal and premotor cortices: motor attention and selection. *Neuroimage* 20 (Suppl 1), S89–S100.
- Schluter, N.D., Rushworth, M.F., Passingham, R.E., Mills, K.R., 1998. Temporary interference in human lateral premotor cortex suggests dominance for the selection of movements. A study using transcranial magnetic stimulation. *Brain* 121 (Pt 5), 785–799.
- Schluter, N.D., Krams, M., Rushworth, M.F., Passingham, R.E., 2001. Cerebral dominance for action in the human brain: the selection of actions. *Neuropsychologia* 39, 105–113.
- Simon, S.R., Meunier, M., Piettre, L., Berardi, A.M., Segebarth, C.M., Boussaoud, D., 2002. Spatial attention and memory versus motor preparation: premotor cortex involvement as revealed by fMRI. *J. Neurophysiol.* 88, 2047–2057.
- Solodkin, A., Hlustik, P., Chen, E.E., Small, S.L., 2004. Fine modulation in network activation during motor execution and motor imagery. *Cereb. Cortex* 14, 1246–1255.
- Stephan, K.M., Frackowiak, R.S., 1996. Motor imagery—anatomical representation and electrophysiological characteristics. *Neurochem. Res.* 21, 1105–1116.
- Stephan, K.M., Fink, G.R., Passingham, R.E., Silbersweig, D., Ceballos-Baumann, A.O., Frith, C.D., Frackowiak, R.S., 1995. Functional anatomy of the mental representation of upper extremity movements in healthy subjects. *J. Neurophysiol.* 73, 373–386.
- Stilla, R., Deshpande, G., LaConte, S., Hu, X., Sathian, K., 2007. Posteromedial parietal cortical activity and inputs predict tactile spatial acuity. *J. Neurosci.* 27, 11091–11102.
- Stinear, C.M., Fleming, M.K., Byblow, W.D., 2006. Lateralization of unimanual and bimanual motor imagery. *Brain Res.* 1095, 139–147.
- Szameitat, A.J., Shen, S., Sterr, A., 2007. Motor imagery of complex everyday movements. An fMRI study. *Neuroimage* 34, 702–713.
- Talairach, J., Tournoux, P., 1988. *Co-planar Stereotaxic Atlas of the Brain*. Thieme, New York.
- Tanaka, S., Inui, T., 2002. Cortical involvement for action imitation of hand/arm postures versus finger configurations: an fMRI study. *Neuroreport* 13, 1599–1602.
- Tanaka, S., Inui, T., Iwaki, S., Konishi, J., Nakai, T., 2001. Neural substrates involved in imitating finger configurations: an fMRI study. *Neuroreport* 12, 1171–1174.
- Venkatraman, V., Payne, J.W., Bettman, J.R., Luce, M.F., Huettel, S.A., 2009. Separate neural mechanisms underlie choices and strategic preferences in risky decision making. *Neuron* 62, 593–602.
- Wen, X., Zhao, X., Yao, L., 2006. Applications of Granger causality model to connectivity network based on fMRI time series. *International Conference on Advances in Natural Computation, Xi'an(CN)*, pp. 205–213.
- Wise, S.P., Boussaoud, D., Johnson, P.B., Caminiti, R., 1997. Premotor and parietal cortex: corticocortical connectivity and combinatorial computations. *Annu. Rev. Neurosci.* 20, 25–42.
- Zeng, L., Chen, H., Ouyang, L., Yao, D., Gao, J.H., 2007. Quantitative analysis of asymmetrical cortical activity in motor areas during sequential finger movement. *Magn. Reson. Imaging* 25, 1370–1375.
- Zhou, Z., Chen, Y., Ding, M., Wright, P., Lu, Z., Liu, Y., 2009. Analyzing brain networks with PCA and conditional Granger causality. *Hum. Brain Mapp.* 30, 2197–2206.